Stochastic Nonlinear Dynamics: How Many Ion Channels are in a Single Neuron?

F. Buchholtz, N. Schinor, and F. W. Schneider*

Institute of Physical Chemistry, University of Wuerzburg, Am Hubland, 97074 Wuerzburg, Germany

Received: May 31, 2001; In Final Form: January 30, 2002

We apply our stochastic cell model to simulate the noisy shape of single neuronal action potentials on the basis of the nonlinear oscillatory Brusselator model. By comparison with the experimental action potentials as measured by Laurent and co-workers in the olfactory system of the locust, we conclude that at least ∼14 000 ion channels in a local neuron (LN) and ∼70 000 ion channels in a project neueron (PN) are responsible for the stochastic appearance of the measured action potentials. Instead of treating the stochastic gating of ionic channels as a multistate Markov process, we use a computer simulation that performs a direct count of all events of each individual reaction step on the basis of their Poisson distributions. Our stochastic analysis is independent of the particular architecture of the neuronal network.

Introduction

A single neuron is not only a simple "integrate and fire" device, but it displays a number of dynamic states in analogy to familiar nonlinear chemical reactions as pertinent experimental data indicate. In fact, this view is not new.[1−7]

In any given neuron, the total number of ion channels is finite. How does this finite number of ion channels affect the appearance of the action potential of a firing neuron? This question has been addressed by several authors who compared the classical Hodgkin−Huxley (HH)[8] equations with a stochastic formulation using random Markov kinetics[7,9−16] which includes the opening and closing of discrete ion channels. In the limit of large numbers of channels, the size of fluctuations becomes small, and the stochastic formulation converges to the continuous deterministic HH description.

Instead of using Markov chains, Langevin, Fokker−Planck or the master equation approach to the HH model, we offer precise computer simulations[17] of a very simple model for the stochastic description of a neuron, namely the Brusselator model.[18] The simple Brusselator shows generic similarities in its nonlinear behavior with the HH model:[27] the bifurcation diagram of the Brusselator is qualitatively similar to that of a HH neuron. Both models show a focal steady state with a subcritical Hopf bifurcation at low applied "currents" followed by an oscillatory region and a supercritical Hopf transition from the oscillatory state to yet another focal steady state in a plot of the membrane potential versus a bifurcation parameter, the applied current, in this case.

Importantly, the FitzHugh−Nagumo[19] model being a reduced version of the HH equations has been shown to be equivalent to a lattice gas model,[20] i.e., a microscopic reaction model that contains nonlinear reaction steps similar to the Brusselator ($2A + A^* \rightarrow 3A$; $2A^* + A \rightarrow 3A^*$, where A is a molecular species and A^* represents its vacancy) in addition to four cyclically coupled catalytic steps. Therefore, the high degree of nonlinearity of the Brusselator is also contained in the HH equations. Because we are interested mainly in an analysis of the noisy shape of an action potential and not in any network properties such as phases or excitatory and/or inhibitory interactions, the use of the much simpler Brusselator model seems to be justified.

The Brusselator contains the strongly nonlinear (autocatalytic) step $2X + Y \rightarrow 3X$. In this work, we equate the X- and Y-particles with the number of open and closed ion channels in a single neuron, respectively. Thus, the closed channels are converted to open channels in a strongly cooperative process catalyzed by the presence of open channels in a second-order autocatalysis. The simple Brusselator does not distinguish between K^+, Na^+, or Ca^{2+} channels. To compare the stochastic cell model with the continuous Brusselator the latter has to be formulated in terms of reaction probabilities.[17] As a result, we shall obtain an estimate of the lower limit of the effective number of ion channels in a neuron which turns out to be comparable with the estimates obtained from conductivity measurements of single ion channels.[5,7,21]

Then the question will arise whether the noisy (stochastic) appearance of the experimental action potentials originates from a finite number of ion channels or from jitter inherent in instrument noise or from both. Obviously, a strong jitter may mimic a small number of particles leading to a lowering of the estimate of the number of ion channels. For a comparison with experiment we have chosen some of the very impressive experiments by Laurent and co-workers[22−25] who studied the dynamic behavior of single neurons in the olfactory system of the locust and the honey bee.

In summary, an odor is represented by the temporal evolution of an ensemble of projection neurons (PN) in the antennal lobe of the animal, and the ensemble shows synchronization as indicated by the existence of an oscillatory local field potential (LFP). Specifically, we focus our attention on a set of intracellular recordings by MacLeod and Laurent[22] from synaptically connected antennal lobe local neurons (LN) and PNs in vivo during a response to a cherry odor (Figure 2a). The LN consists of a dendritic tree without an axon (Figure 2a), which may be the reason why the generated LN potentials are relatively broad and of low amplitude. Inhibitory coupling of the LN to the PNs results in the establishment of coherence in the firing of many PNs which are phase shifted relative to the LN potential.

10.1021/jp0120662 CCC: $22.00
Published on Web 04/24/2002

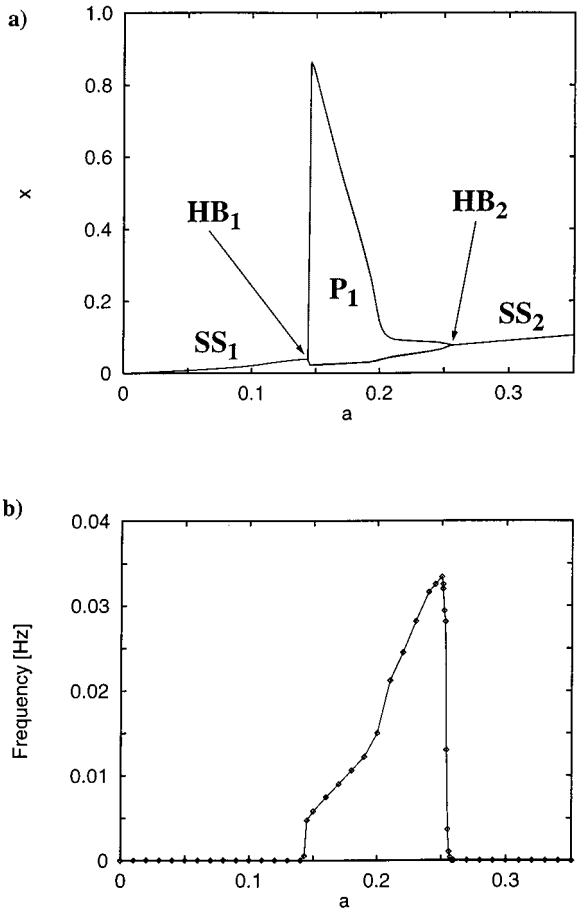

Figure 1. (a) Bifurcation diagram of the probability model for a PN (eqs 5,6) shows a focal steady state (SS_1) (or excitable state), a subcritical Hopf bifurcation (HB_1), period one (P_1) oscillations and a focus with a supercritical Hopf bifurcation (HB_2) and a focal steady state (SS_2); amplitude as a function of the bifurcation parameter *a*. For high *f*-values the time series of the probability model will approach those of the "normal" Brusselator. A PN has the parameters $f = 5$, $b = 0.80$, $c = 0.66$, and $g = 1.5 \times 10^{-3}$; (a LN (not shown) has $f = 5$, $b = 0.25$, $c = 0.20$ and $g = 1.6 \times 10^{-4}$); the PN oscillation amplitude shows a sharp maximum. (b) Frequency dependence of a PN in part a. The frequency displays a maximum close to HB_2.

Interestingly, coherence is lost when picrotoxin (PCT), an antagonist of GABA receptors, is injected. The LFP flattens out because PCT specifically blocks the fast inhibitory synapses between local and projection neurons, whereas the signatures of the individual PNs were unchanged except for a somewhat increased firing rate. Using a recurrent neuronal network of 80 projection neurons and a nonoscillating local neuron[27] we have achieved good agreement with the above experiments on the basis of HH neurons including the short-term memory effect in 10 repeated presentations of a given odor.

The present stochastic analysis uses the appearance of two types of oscillations: the "broad" LN oscillations of low amplitude and the "sharp" spikes of a firing projection neuron. The stochastic appearance of the "broad" LN potential can be readily characterized whereas that of a sharply firing PN mainly consists of a steep rise and decline of the electric potential including a small "noisy" base. In our stochastic analysis, we assume that the particular structure of the neuronal network has a negligible effect on the stochastic character of an individual neuronal oscillation and that we can therefore use oscillating "Brusselators" for a LN and a PN.

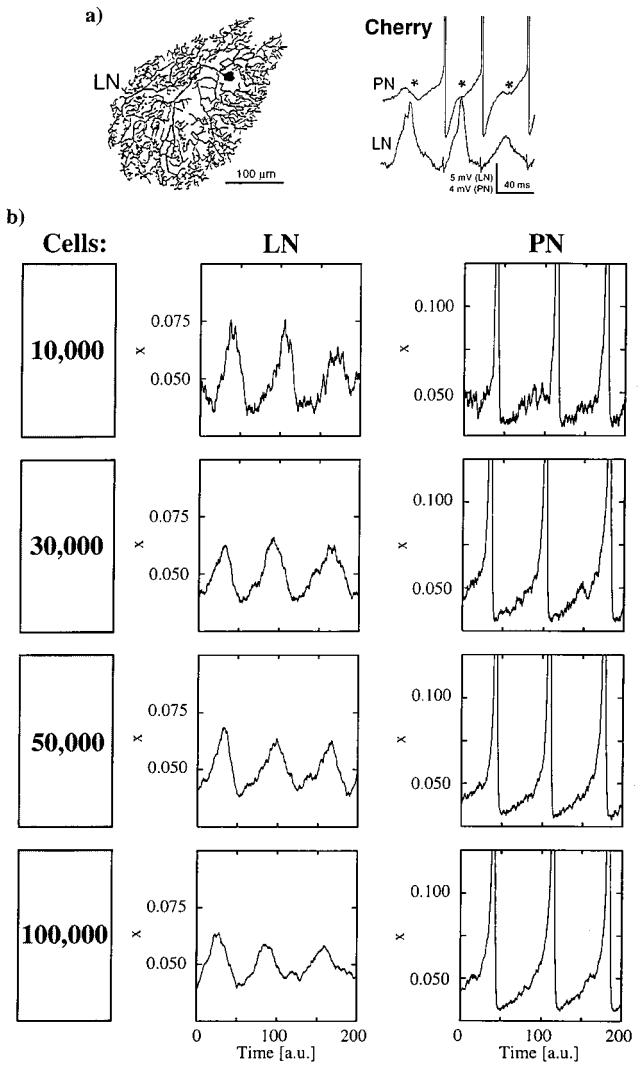

Figure 2. (a) Camera lucida drawing of a local neuron and simultaneous intracellular recordings from a LN and a postsynaptic PN during a response to an odor (cherry) in a locust.[22] PN spikes are clipped. With kind permission of the authors. (b) Excerpted time series for a PN and a LN using the stochastic cell model for $n = 10\,000$, 30 000, 50 000 and 100 000 mathematical cells. Reasonable agreement by comparison with the experimental action potentials (Figure 2a) is seen for ~50 000 (~14 000 ion channels) virtual cells for a LN and for ~100 000 (~70 000 ion channels) virtual cells for a PN, at an applied current of $a = 0.21$ for a PN and $a = 0.05$ for a LN. The phase relations between the LN and the PNs in a recurrent network have been treated elsewhere.[27] As the number of virtual cells increases, the inherent natural noise decreases and the amplitudes of the LN-oscillations decrease as a consequence.

Brusselator. The Brusselator has 5 steps:

$a \rightarrow X$

$X \rightarrow Y + F$ (rate coefficient b)

$2X + Y \rightarrow 3X$

$X \rightarrow D$ (rate coefficient c)

$Y \rightarrow E$ (rate coeffient g)

In the present neuronal application, the first step provides a (low) background of open ion channels (X) and the second step represents the spontaneous closing of open channels to form closed ion channels (Y). The strong "cooperativity" of the mechanism is expressed by the third step in which the closed channels are converted to open channels in a process which is autocatalyzed by the presence of some open channels. The fourth step represents the natural lifetime of the open state. We added the fifth step in order to also account for the lifetime of the

closed channels. The species F, D, and E areproducts, and they do not appear explicitly in the kinetic differential equations for X (eq 1) and Y (eq 2). The values of *b*, *c*, and *g* are identical with those in the following probability model (Figure 1) and in the stochastic cell model (Figure 2b). The differential equations for the above two-variable Brusselator are

$$\frac{dX}{dt} = a + X^2Y - (b + c)\,X \tag{1}$$

$$\frac{dY}{dt} = bX - X^2Y - gY \tag{2}$$

We choose the specific rate coefficients *b*, *c*, and *g* (in Figure 1a) in such a way as to closely reproduce the general shape of the oscillations of a LN and a PN for specific values of *a*, where *a* represents the current applied to a LN or a PN.

Probability Model of the Brusselator. It is important to reduce the concentrations *X* and *Y* to values below unity for a comparison with the stochastic cell model. For this reason the probability model introduces the scaling factor *f*. Low values of f ($< \sim 5$) may have a large effect on the calculated frequencies or firing patterns when compared with the "normal" Brusselator; *f* also affects the amplitudes of the oscillations and the absolute values of the steady-state concentrations. However, in all calculations *f* is kept constant. Thus $x = X/f$ and $y = Y/f$, where *x* and *y* are the scaled concentrations of *X* and *Y*, respectively, and

$$\frac{dx}{dt} = a/f + f^2x^2y - (b + c)\,x \tag{3}$$

$$\frac{dy}{dt} = bx - f^2x^2y - gy \tag{4}$$

The resulting term f^2x^2y arises from the reaction step $2X + Y \rightarrow 3X$. To calculate the joint probability of finding at least one *y*-particle ($P_{1(y)}$) and two *x*-particles ($P_{2(x)}$) in a virtual cell we use the Poisson distribution

$$P = \frac{y^m}{m!}e^{-y}$$

where *m* is the number of *y*-particles and *y* is the average number of *y*-particles.

Thus

$$P_{1(y)} = ye^{-y} + \frac{y^2}{2!}e^{-y} + \frac{y^3}{3!}e^{-y} + \ldots = (e^y - 1)e^{-y} = 1 - e^{-y}$$

and

$$P_{2(x)} = \frac{x^2}{2!}e^{-x} + \frac{x^3}{3!}e^{-x} + \ldots = (e^x - x - 1)e^{-x} = 1 - x\,e^{-x} - e^{-x}$$

The joint probability P_R is the product

$$P_R = P_{1(y)}\,P_{2(x)} = 1 - e^{-y} + (x + 1)\,(e^{-x-y} - e^{-x})$$

Equations 3 and 4 may now be written as a "probability model"

$$\frac{dx}{dt} = \frac{a}{f} + 2f^2P_R - (b + c)\,x \tag{5}$$

$$\frac{dy}{dt} = bx - 2f^2P_R - gy \tag{6}$$

where the probability P_R approaches $x^2y/2$ for low values of *x* and *y* as shown by a series expansion up to the third power. The time series of the probability model will approach those of the "normal" Brusselator for large values of *f* (eqs 1 and 2). The probability model always leads to continuous and smooth action potentials, which provide no information about the number of individual ion channels involved.

Stochastic Cell Model of the Brusselator. The cell model is totally stochastic; it randomizes each single reaction step. Thus it may be generally formulated to describe the effect of inherent fluctuations stemming from very few particles that react according to any multistep nonlinear kinetic mechanism. The cell model is based on individual reaction steps. Therefore, the Brusselator is directly applicable. The number of *X*-particles and *Y*-particles is related to *x* and *y* of the probability model by $i_x = xn$ and $i_y = yn$, respectively, where *n* is the number of virtual cells. The number of virtual cells containing at least one *Y*- and two *X*-particles simultaneously is written as *j*. Thus, *j* corresponds to P_R in the probability model (eqs 5 and 6). The two difference equations for Δi_x and Δi_y are

$$\frac{1}{2f^2}\cdot\frac{\Delta i_x}{\Delta t} = \frac{n_a}{2f^3} + j - \frac{bi_x}{2f^2} - \frac{ci_x}{2f^2} \tag{7}$$

and

$$\frac{1}{2f^2}\cdot\frac{\Delta i_y}{\Delta t} = \frac{bi_x}{2f^2} - j - \frac{gi_x}{2f^2} \tag{8}$$

The computer simulations proceed as follows:

First, all cells are cleared of all particles. Then a given number (i_x and i_y) of *X* and *Y* particles are distributed randomly over *n* virtual cells using a random number generator. The number of cells containing at least one *Y*- and two *X*-particles simultaneously are counted and set equal to *j*. The values for the terms of $na/2f^3$, $bi_x/2f^2$, $ci_x/2f^2$ and $gi_y/2f^2$ are directly calculated and treated as mean values of individual Poisson distributions whose width is determined by the square root of the mean. For each term a random number generator picks a number within the width of the Poisson distribution. Thus, all possible events in each reaction step are randomized. The resulting terms are added or subtracted according to eqs 7 and 8 generating a new value for Δi_x and Δi_y. This procedure is repeated for every time interval $\Delta t = 1/2f^2$.

Translated into the neuronal picture the time series for *X* (open) and *Y* (closed) channels are obtained for a constant number of virtual cells *n*. The total number of ion channels for a given *n* is calculated as the sum of the numbers of *X*- and *Y*-channels in all virtual cells averaged over the calculated time span. The calculations are repeated for different cell numbers n and compared by inspection with the experiment. A more quantitative measure for the fit may also be used.

A virtual cell is considered as a mathematical entity and not as a biological cell. A low number of virtual cells implies a low number of *X* and *Y* particles since *x* and *y* should be below unity. A small positive fluctuation in the current is sufficient to carry the system from the sub-threshold focal steady state across threshold into the oscillating region provided that the system is very close to the Hopf bifurcation. A similar argument applies to superthreshold inputs which will show "missing" oscillations[10] for small fluctuations close to the (unresolved) inversion point where the limit cycle becomes unstable and the system changes into its focal steady state. This extreme sensitivity toward small

TABLE 1: Stochastic Cell Model for the Brusselator[a]

time	0.02	0.04	0.06	66.32	66.34	66.36
i_x	1500	1500	1489	14558	14551	14609
i_y	7500	7513	7544	12434	12289	12103
j	12	1	4	379	405	388
na/2f^3	40.000	40.000	40.000	40.000	40.000	40.000
Poisson	37.365	39.971	44.456	43.453	48.236	37.863
bi_x/2f^2	24.000	24.000	23.824	232.928	232.816	233.744
Poisson	25.106	32.404	25.311	234.171	218.597	234.297
ci_x/2f^2	19.800	19.800	19.655	192.166	192.073	192.839
Poisson	24.427	19.332	24.955	195.296	176.535	201.106
gi_y/2f^2	0.2250	0.2254	0.2263	0.3720	0.3687	0.3631
Poisson	0.2956	0.2578	−0.2394	0.5347	−0.2047	1.4299
Δi_x	0	−11	−2	−7	58	−10
Δi_y	13	31	22	−145	−186	−155

[a] Excerpts of a stochastic calculation of eqs 7 and 8 for a PN (n = 50 000 virtual cells). Initial conditions ($t = 0$) have been chosen as $i_x = 1500$ and $i_y = 7500$; (corresponding to $x = 0.03$ and $y = 0.15$ in the probability model), $\Delta t = 0.02$ au; all terms of eqs 7 and 8 are listed for $a = 0.20$, $b = 0.80$, $c = 0.66$ and $g = 1.5 \times 10^{-3}$ in the left column as mean values together with the values picked randomly from the Poisson distributions of each term. The first three columns give the resulting Δi_x and Δi_y at the start for three successive Δt for a low PN potential with small i_x and i_y. The fourth to sixth columns depict an arbitrarily selected time window to show what happens near the PN maximum; here, the PN potential (proportional to i_x and i_y) is relatively large at 66.32, 66.34 and 66.36 time units, respectively, where all random terms involving i_x and i_y are substantially larger than at the start. The strong stochastic behavior is clearly evident. Only the respective random terms called "Poisson" are used in the calculations.

fluctuations obviously disappears when the applied current is far from the Hopf bifurcation.

Results and Discussion

Bifurcation Diagram for the Probability Model. A bifurcation diagram conveniently summarizes the total dynamic behavior of a mechanism. It has been calculated for the probability model (eqs 5 and 6) with $f = 5$, $b = 0.80$, $c = 0.66$, and $g = 1.5 \times 10^{-3}$ (Figure 1) which is regarded as the bifurcation diagram of a single projection neuron PN, where a is the applied current acting as the bifurcation parameter. At a subcritical Hopf bifurcation (HB_1), a focal steady state (SS_1) is followed by a region of sustained oscillations ($0.145 < a < 0.254$). For the chosen parameters, the threshold for firing is the sudden onset of oscillations at the subcritical Hopf point at $a \simeq 0.145$, whose narrow width is not resolvable. The oscillation frequency increases with increasing values of a ($0.145 < a < 0.254$) (Figure 1b), whereas the amplitude of the oscillation decreases drastically (Figure 1a). A supercritical Hopf bifurcation is observed at a high value of a ($= 0.254$) followed by a focal steady state (SS_2), which, however, is not involved in the present calculations.

The bifurcation diagram for the LN is somewhat similar (not shown). Although similar frequencies are obtained, the LN amplitudes are smaller and the potentials are broader than those of the PNs for the values of a used in the time series, as required by experiment and as expressed by a different set of the chosen parameters: $f = 5$, $b = 0.25$, $c = 0.20$ and $g = 1.6 \times 10^{-4}$.

Computer Simulations of the Stochastic Cell Model. To determine the approximate number of ion channels (equal to the average sum of all X and Y particles), we did cell model calculations using parameters identical with the probability model with cell numbers ranging from $n = 10\,000$ to 100 000 cells for a LN and a PN. Excerpts of a stochastic calculation ($n = 50\,000$) are shown for illustration purposes at $t = 0$ and at the peak of a PN potential (Table 1).

TABLE 2: Results of Computer Calculations for the Stochastic Cell Model for the Time Series Shown in Figure 2b[a]

	cells	i_x	i_y	ion channels
LN	10000	492.823	2312.6	2805.43
	30000	1480.26	6860.8	8341.06
	50000	2490.5	11486.6	13977.1
	100000	4990.34	23015.9	28006.2
PN	10000	594.913	6350.9	6945.81
	30000	1810.02	19244.5	21054.6
	50000	2936.28	31420.2	34356.5
	100000	6007.83	64435.2	70443.2

[a] Values for i_x, i_y and ion channels ($i_x + i_y$) represent numbers which have been averaged over a time span of 200 au

The stochastic nature of the resulting time series is clearly evident. It is seen, that the synaptic input a is not the largest source of noise. Every single term involving the finite number of open and closed ion channels i_x and i_y, respectively, contributes substantially to the stochastic behavior. Thus, it is the finite and changing number of reacting particles in the highly nonlinear step $2X + Y \rightarrow 3X$ representing the opening of channels which is responsible for the noisy appearance of the LN and PN time series (Figure 2b and Table 2).

The time series of LN and PN neurons in Figure 2b bear a close resemblance to the experimental (Figure 2a) potentials. For a LN the visual fit regarding the noisy appearance of the potential seems closest for 50 000 virtual cells corresponding to about 14 000 ion channels. The latter number is obtained by calculating the sum of all i_x and i_y particles and averaging over the time span of the calculation. For the largest virtual cell number ($n = 100\,000$) the simulated LN potential looks to be smoother than in the experiment (Figure 2a). Experiments[22] have shown that the LN potential is subthreshold and relatively wide and low in amplitude. Furthermore, a LN is a cell with a dendritic tree but without an axon (Figure 2a). This situation may justify the lower number of ion channels than that found in a PN: The visual fit with a PN is closest for a larger number of mathematical cells, namely about 100 000, corresponding to about 70 000 ion channels as the total number of ion channels in a PN as a lower limit. However, a visual inspection with the experiments can only give an approximate fit.

Earlier molecular dynamics calculations[29] have also shown that a strong nonlinearity is the underlying cause for the high sensitivity toward even small fluctuations close to the turning point of a bistability involving the step $2X + Y \rightarrow 3X$ where the phenomenon of critical slowing down has been observed even for a finite number of particles.

It is seen that the simple Brusselator does not reproduce the "dip" caused by an "afterhyperpolarization"[22] of a PN (Figure 2b) indicating that the Brusselator is a gross simplification for a neuron, of course. Thus, for lower virtual cell numbers and low number of particles (ion channels) the calculated action potentials become "noisy", which is particularly evident in the LN potential, whereas the PN potentials reveal their noise mainly at the base. Thus one observes a gradual transition from a stochastic ("noisy") to a continuous ("smooth") behavior as expected as the number of virtual cells (and ion channels) is increased (Figure 2b).

Instrumental Noise. Any contribution of further instrument noise will decrease the lower limit of the number estimate of ion channels. We assume that the measured action potentials of single neurons represent raw and unfiltered data except in the case of the (averaged) local field potential which, however, is not used here for any estimate. Thus, our estimate of the number of ion channels represents an approximate lower limit.

Channel Densities. On the basis of the size of the soma of a LN (Figure 2a) (radius ~5 μm), one may calculate about ~40 ion channels per square micrometer (14 000 channels divided by the surface area of a sphere), which is well within the densities of ion channels reported in the literature.[7,21,28] However, our densities are speculative because they have been calculated without any contributions from the dendrites which may form tree-like structures of large surface areas in a LN. The total number of ion channels may also be affected, since the currents coming from various dendrites may "add" nonlinearly.[32] In our rough estimate of the lower limit of the number of ion channels such important details may not be visible.

Models. In the stochastic cell model no assumptions about the particular geometries of the cells or particles are necessary. The number of ion channels, given as a lower limit in this work, represents the total number of open and closed ion channels averaged over a time span at a certain applied current. We note that our chosen parameters for a LN and PN are independent of any network architecture. In independent work,[27] we have assumed that a LN of the locust does not oscillate intrinsically but that is is synaptically driven by the sum of many PN potentials which are made coherent through inhibitory synaptic LN→PN interactions. Still, we regard a LN as self-oscillatory here since we are interested only in the stochastic appearance of its potential. A PN, however, does oscillate intrinsically in the olfactory system of the locust. Whatever its particular physical interpretation, the Brusselator model may be generalized to many other relevant "selforganizing" processes showing threshold properties.

Fluctuations. In general, fluctuations are always "large" when the neuron is in its "excitable" focal steady state close to the Hopf bifurcation. However, when an odor is registered and the applied current sweeps rapidly from zero across the Hopf bifurcation into the oscillating region, the dynamics will be characterized by transient behavior[27] and the effective threshold is no longer "static". There are other interesting details such as the so-called time-to-amplitude conversion[30] which triggers an action potential earlier if the system starts closer to the "threshold" than if it starts farther away. Thus, the neuronal signatures in a network represent transients which depend strongly on initial and final conditions as well as on the rate of change of the applied current a. Some of these issues are discussed elsewhere.[27]

Comparison with Markov Calculations. In Markov calculations of the HH model, the assumption is made that transitions occur with equal probabilities between all four respective m^3h-states of a Na^+-channel and nonlinearity enters through the relation between conductance and the membrane voltage. Furthermore, a single LN or PN is spatially distributed which may be generally treated quantitatively.[31] It seems that the relative numbers for the ion channels obtained from the Markov calculations are comparable with those of the present stochastic cell model which considers the whole neuron (and not only a small patch) to contribute to the action potential of intracellular recordings.

Conclusions

The stochastic cell model predicts about ~14 000 ion channels in a LN and about 70 000 ion channels in a PN (without information of their spatial distribution) as a lower limit of ion channels that lead to a similar stochastic appearance of single potentials as in the experiment. Each individual process is randomized in the computer simulations. The cell model based on the Brusselator provides only a gross measure because it contains a number of unknowns which must be fitted. Also, it does not distinguish between the types of ion channels, such as Na^+ or K^+ channels. Despite these shortcomings the stochastic Brusselator predicts similar orders of magnitude in the numbers of ion channels as those obtained from entirely different experimental methods.[7,21,28]

We conclude that the highly cooperative transitions between small numbers of closed and open ion channels determine the noisy appearance of an action potential of a single neuron. It is perhaps surprising that a relatively simple model mechanism such as the Brusselator seems to be sufficiently nonlinear to reproduce the noise in single neuronal potentials.

Acknowledgment. We dedicate this work to Professor Friedrich Dörr on the occasion of his 80th birthday.

Supporting Information Available: The code for the computer calculations is available free of charge via the Internet at http://pubs.acs.org

References and Notes

(1) Rinzel, J. In. *Ordinary and Partial Differential Equations: Proceedings of the 8th Dundee Conference*; Sleeman, B. D., Jarvis, R. J., Eds.; New York: Springer **1985**, *1151*, 304.

(2) Hanyu, Y.; Matsumoto, G. *Physica* **1991**, *D49*, 198.

(3) Buchholtz, F.; Golowasch, J.; Marder, E.; Epstein, I. R. *J. Neurophysiol.* **1992**, *67*, 332.

(4) Abbott, L. F. *Quart. Rev. Biophys.* **1994**, *27*, 291.

(5) Arbib, M. A., Ed. *The Handbook of Brain Theory and Neural Networks*; MIT Press: Cambridge, Massachusetts, 1994.

(6) Wang, X.-J.; Rinzel, J. In. *The Handbook of Brain Theory and Neural Networks*; Arbid, A., Ed.; MIT Press: Cambridge, Massachusetts, 1996.

(7) Koch, C. *Biophysics of Computation: Information Processing in Single Neurons*; Oxford University Press: New York, 1999.

(8) Hodgkin, A. L.; Huxley, A. F. *J. Physiol.* **1952**, *117*, 500.

(9) Neher, E.; Stevens, C. F. *Annu. Rev. Biophys. Bioeng.* **1977**, *6*, 345.

(10) Strassberg, A.; De Felice, L. J. *Neural Comput.* **1993**, *5*, 843.

(11) DeFelice, L. J.; Goolsby, W. N. In. *Fluctuations and Order: The New Synthesis.* Millonos, M., Ed.; Springer, New York, 1996. DeFelice, L. J.; Isaac, A. *J. Stat. Phys.* **1992**, *70*, 339.

(12) Clay, J.; DeFelice, L. J. *Biophys. J.* **1983,** *42*, 151.

(13) Chow, E. C.; White, J. A. *Biophys. J.* **1996**, *71*, 3013.

(14) White, J.; Budde, T.; Kay, A. *Biophys. J.* **1995**, *69*, 1203.

(15) Skaugen, E.; Walløe, L. *Acta Physiol. Scand.* **1979**, *107*, 343.

(16) Schneidman, E.; Freedman, B.; Segev, I. *Neural Comp.* **1998**, *10*, 1679.

(17) Buchholtz; F.; Schneider, F. W. In. *Spatial Inhomogeneities and Transient Behavior in Chemical Kinetics*; Gray, P., Nicolis, G., Baras, F., Brockmans, P., Scott, S. K., Eds.; Manchester University Press: Manchester, UK, 1992.

(18) Prigogine, I.; Lefever, R. *J. Chem. Phys.* **1968**, *48*, 1695.

(19) FitzHugh, R. *Biophys. J.* **1961**, *1*, 445. Nagumo, J.; Arimoto, S.; Yoshikawa, Y. *Proc. IRE* **1962**, *50*, 2061.

(20) Malevanets, A.; Kapral, R. *Phys. Rev.* **1997**, *E55*, 5657.

(21) Hille, B. *Ionic Channels of Excitable Membranes*, 2nd ed.; Sinauer Associates: Sunderland, MA, 1992.

(22) MacLeod, K.; Laurent, G. *Science* **1996**, *274*, 976.

(23) Wehr, M.; Laurent, G. *Nature* **1996**, *384*, 162.

(24) Stopfer, M.; Bhagavan, S.; Smith, B. H.; Laurent, G. *Nature* **1997**, *390*, 70.

(25) Stopfer, M.; Laurent, G. *Nature* **1999**, *402*, 664.

(26) Stopfer, M.; Wehr, M.; MacLeod, K.; Laurent, G. In *Insect Olfaction*; Hanssen, B. S., Ed.; Springer-Verlag: Berlin, Heidelberg, NewYork, 1999,

(27) Schinor, N.; Schneider. F. W. *PCCP* **2001**, *3*, 4060.

(28) Alberts, B.; Bray, D.; Lewis, J.; Raff, M.; Roberts, K.; Watson, J. D. *Molecular Biology of the Cell*, 3rd ed.; Garland Publishing: New York, 1994.

(29) Heinrichs, M.; Schneider, F. W. *Ber. Bunsen-Ges.* **1983**, *87*, 1195.

(30) Hopfield, J. J. *Nature* **1995**, *376*, 33.

(31) Mainen, Z. F.; Sejnowski, T. J. *Nature* **1996**, *382*, 363.

(32) Koch, C.; Segev, I. *Nature Neurosci.* **2000**, *3*, 1171.